Water Resources and Industry 3 (2013) 23–34

Contents lists available at SciVerse ScienceDirect

Water Resources and Industry

journal homepage: www.elsevier.com/locate/wri

Treatment of highly concentrated dye solution by coagulation/flocculation–sand filtration and nanofiltration

A.Y. Zahrim [a,*], N. Hilal [b]

[a] Chemical Engineering Programme, School of Engineering and Information Technology, Universiti Malaysia Sabah, Jalan UMS, 88400 Kota Kinabalu, Sabah, Malaysia
[b] Centre for Water Advanced Technologies and Environmental Research (CWATER), College of Engineering, Swansea University, Swansea SA2 8PP, UK

ARTICLE INFO

Article history:
Received 20 March 2013
Received in revised form
7 May 2013
Accepted 16 June 2013

Keywords:
Coagulation/flocculation
Nanofiltration
Acid black 210
Sand filtration
Decolorization

ABSTRACT

Treatment of highly concentrated C.I. Acid Black 210 dye solution using direct coagulation/flocculation–sand filtration (without sedimentation) and nanofiltration has been investigated in this paper. It was found that none of the treatments were able to fully decolourise the dye solution, but nanofiltration permeate quality was better, based on colour, residual dye, pH, and total organic carbon. The red colour for the sand filtration filtrate might be due to the formation of stable aluminium–sulphonic acid complexes. The sand filtration breakthrough after coagulation/flocculation is estimated at around 45 min. For nanofiltration of highly concentrated dye (>1000 mg/l), the separation factor analysis had confirmed that the mechanism of dye molecules attached to the membrane surface is irreversible adsorption.

1. Introduction

Colour that appears in industrial wastewater could be due to dye(s) application [55], plant component i.e. lignin, tannin as well as its biodegradation product e.g. melanoidin [5]. The presence of colourant in surface water is aesthetically undesirable and causes disturbance of the aquatic biosphere due to reduction of sunlight penetration and depletion of dissolved oxygen. Some colourants are toxic

* Corresponding author. Tel.: +60 883 20000; fax: +60 883 20348.
E-mail address: zahrim@ums.edu.my (A.Y. Zahrim).

2212-3717
http://dx.doi.org/10.1016/j.wri.2013.06.001

and mutagenic and have the potential to release the carcinogenic amines. Due to their recalcitrant properties, colourants can also contribute to the failure of biological processes in wastewater treatment plants [55]. In some applications, coloured treated water is also not suitable for water reuse.

As the legislation related to environment is becoming tougher in many countries due to an increase of public awareness, decolourisation of industrial wastewater requires much effort from scientists and engineers to sustain the related industries. Generally, there are two decolourisation methods: by destruction of colourant molecules (e.g. chemical oxidation and bio-oxidation) and the other is by separation of colourants from water (e.g. coagulation/flocculation, sand filtration and membrane separation). As they are likely to be effective methods for decolourisation [56] and the concentrated colourant could be turned into a useful product (e.g. compost [38] and brick [6]), two separations processes i.e. direct coagulation/flocculation–sand filtration (CF–SF) and nanofiltration (NF) have been used in this study.

Slow sand filtration is known as a simple option for water treatment and has a filtration rate of about 0.1–0.5 m^3/m^2 h [46]. Due to dyes' high solubility, flocs that are generated from the coagulation/flocculation of soluble colourants are difficult to settle [29]. After coagulation/flocculation, sand filtration could remove colourant flocs by attaching them to the sand grain or to previously retained flocs (ripening).

Performance of slow sand filtration depends on the chemicals used for pre-treatment. Addition of a metal coagulant has been reported to improve the removal of colour (measured as absorbance at 254 nm), turbidity and phosphorus [19]. Aluminium sulphate is reported to have minimal head lost compared to $AlCl_3$ and $FeCl_3$ during direct coagulation-sand filtration of effluent from extended aeration treatment [19]. However, the application of aluminium based coagulant alone is not sufficient during long term experiments. Polymer (e.g. low cationic polyacrylamide) was reported to enhance direct sand filtration performance by minimising the decline of turbidity removal before sand filter became clogged [17]. It has also been reported that alum+cationic polymer increases the filter run time and increases the flow-rate [46].

In order to reduce the cost, direct coagulation-sand filtration is preferable to coagulation-sedimentation-sand filtration. It has been reported that coagulation-sedimentation-sand filtration has double capital cost than direct coagulation-sand filtration [2]. Several studies on colourants removal via coagulation-sedimentation-sand filtration have been reported [41,10,56] but published studies on direct coagulation/filtration-sand filtration for coloured wastewater is lacking. Furthermore, greater water recovery is possible by removing the sedimentation step.

Nanofiltration (NF) has been recognised as a key tool for wastewater recycle/reuse. Its application for treatment of coloured wastewater have been reported by several investigators [15,45,11,7,26,57]. Nanofiltration (NF) is positioned between reverse osmosis (RO) and ultrafiltration (UF) and its permeability is around 1.5–30 l/m^2 h bar. Nanofiltration membranes carry quite distinctive properties such as pore size (1–5 nm) and surface charge density which influences the separation of various solutes. However, some studies have reported that nanofiltration was unable to produce colourless permeate [55].

The objective of this study is to investigate the performance of CF–SF and NF processes towards decolourisation of C.I. Acid Black 210 dye solution. Due to its extensive application in industry, the treatment of C.I. Acid Black 210 dye was subjected to few studies e.g. chemical oxidation [18], biological treatment [37,32], coagulation/flocculation [54], coagulation-sedimentation-sand filtration [56] and direct nanofiltration [57].

2. Methodology

2.1. C.I. Acid Black 210 dye

The Durapel Black NT (DBNT) dye (contain $>30\%$ C.I. Acid Black 210 dye) was purchased from Town End (Leeds) plc, (United Kingdom) and used without further purification. Sodium sulphate generally used as diluents (personal communication with Dr Adrian Hayes, Technical Director, Town End (Leeds) plc,). A dye mass of 20 g in powder form was dissolved in Milli-Q Plus, 18.2 MΩ cm (Millipore) water to make 5 l solution at a concentration of 4000 mg/l [25,54,56]. The colour of dye solution is visible at minimum concentration of 10 mg/l.

2.2. Coagulation/flocculation–sand filtration study

For direct sand filtration study, the sand grain was fixed at 0.3–0.6 mm based on the previous findings [56] and height about 350 mm. At this condition, the clean filtration rate should be ensured to be around 1.0 m^3/m^2 h. Otherwise, more sand needs to be added to the column. This is because sand size distribution might be wider. The solution after coagulation was fed slowly (about 40 ml in every 5 min). Coagulation/flocculation procedures have been described in details elsewhere [54,25]. The coagulant and flocculant aid used is aluminium sulphate and low-medium molecular mass poly-diallyl-dimethyl ammonium chloride (polyDADMAC), respectively. Normally after each experiment, the blend of sand-flocculated dye would strongly bind towards the glass wall. Thus, to clean the sand column, these steps were followed: (a) remove the microsieve, supporter and marbles. (b) 100 ml of 0.1 M NaOH was fed following 100 ml of Milli-Q water.

2.3. Nanofiltration membrane—AFC80

The NF membrane used was commercially sourced AFC80 (Paterson Candy International Ltd., UK). The AFC series are thin-film composite membranes with a polyamide active film. This film is formed from an aliphatic amide for AFC80. On the basis of the chemistry used, the membrane is expected to have free acid groups and a net negative charge, though each may have some free amine groups present. Bowen and Doneva [12] reported that the mean pore diameter for AFC80 was 0.68 nm while Warczok et al. [48] reported the value was 3.51 nm. The pure water permeability is around 2.8–3.1 l/m^2 h bar.

2.4. Tubular membrane system

The tubular membrane system was designed by CARDEV Ltd. [22] with further modifications carried out on the system. The modified system consists of a feed tank (5 l working volume), pump, and membrane housing (Fig. 1). The maximum inlet pressure is 5.2–5.3 bar and the system automatically shuts down if the pressure exceeds 5.3 bar. The inlet pressure is controlled by an outlet valve. This unit is fitted with tubular nanofiltration membranes with inner diameter of 1.27 cm and effective length of 28.6 cm. Thus, the calculated area of membrane tube is around 0.0114 m^2. In this system, the retentate is sent back to the tank. The pump used is from Mono Pump Ltd., Manchester model CMM253/H13F and delivers a maximum transmembrane pressure around 4.3 bar. The pump is fitted with a motor from Brook Compton Ltd, Doncaster Model KP 7575. At the maximum inlet pressure, the maximum flow rate measured is 1 m^3/h.

Fig. 1. Tubular nanofiltration system.

2.5. Procedure to determine normalised permeation flux, product permeate quality and irreversible fouling factor

The procedures followed for the determination of normalised permeation flux, product permeates quality and irreversible fouling factor are outlined as:

1. The membrane was soaked in RO water for 24 h before the first permeation test with RO water. The pump is switched on at maximum outlet valve opening for 2 min after placing 5 l RO water.
2. The valve is slowly reduced until it reaches highest "unsteady" inlet pressure (inlet: 5.5 bar, outlet: 4.0 bar). After maximum inlet pressure, reduction of valve opening causes system to automatically shut down.
3. The system is then left for at least 2 h to minimise the compaction effect. Permeate and retentate are returned to the feed tank.
4. The outlet valve is then opened again to get the desired inlet pressure.
5. The pure water flux (PWF) is determined by changing the inlet valve. The system is left until steady state (50 min). The permeate volume for 20 min operation is measured. Temperature (θ) was measured every 10 min. A minimum of three points at various transmembrane pressures were obtained. The membrane permeability was determined by plotting pure water flux (PWF) against transmembrane pressure.
   The transmembrane pressure (TMP) calculated as:

$$\Delta P = \frac{\text{Inlet pressure} + \text{Outlet pressure}}{2} \tag{1}$$

   Normalised pure water permeation flux (J_{25}) is determined using the temperature correction as stated by [1]:

$$J_{25} = J_{\theta} \exp\left(0.0239(25-\theta)\right) \tag{2}$$

6. The pump is switched off and the RO water is then replaced with dye solution (5 l) and the system is left for 50 min to achieve steady state condition. The zero time was begun after 50 min.
7. The UV/vis absorbance, pH and conductivity of permeate were taken at time 20, 40, 60, 80, 100 and 120 min after steady state condition was reached. The permeate was returned, after each analysis, to the feed tank to maintain initial dye concentration.
8. After collecting sample at 120th minutes, about 30 ml of permeate was collected, kept at 4 °C and was analysed for TOC.
9. The pump is then switched off and the dye solution was replaced with the tap water (approximately 10 l). The pump was set at the lowest transmembrane pressure available (maximum outlet valve opening). Both retentate and permeate were discarded.
10. The pump was switched off and tap water was replaced with RO water. The pump is set at the lowest transmembrane pressure (maximum outlet valve opening). Both retentate and permeate are returned to the feed tank and were operated for one hour. The system then was left overnight.
11. The membrane permeability was determined as step (5). The irreversible fouling factor defines as IFF was determined as [52]:

$$\frac{\text{Initial membrane permeability} - \text{Membrane permeability after cleaning with water}}{\text{Initial membrane permeability}} \times 100\% \tag{3}$$

2.6. Chemical cleaning

Before dismantling the membrane, about 10 l of 0.1 mM NaOH (pH 10.30) was passed through the system without returning the retentate. The system was rinsed by about 10 l RO water. The main purpose of this procedure is to minimise the dye stain attached on the surface of tubing/pump.

Cleaning of membrane is carried out by submerging the membrane in the solution by following the sequence: 0.01 M HNO_3 (pH 1.94), 0.0001 M NaOH (pH 10.30) and RO water for 60 min each. The water permeability is then measured again. If the pure water permeability is greater than 1.5 l/m^2 h bar; no membrane replacement is implemented. Then the membrane is dismantled and stored in 20% glycerol (ACROS Organic)+1% sodium metabisulfite (ACROS Organic) solution to prevent biological growth on the surface of the membrane [52].

2.7. Physicochemical analysis

The pH and conductivity reading were measured using a Jenway 3540pH/conductivity metre. The calibration was carried out daily at 20 °C. The buffer solutions (pH 4, pH 7 and pH 10) for pH metre calibration were supplied by Fisher Scientific, U.K. Residual concentration of dye (without filtering or centrifuging) was analysed with a UV/vis-spectrophotometer, (UVmini-1240, Shimadzu) by measuring the absorbance (315 nm). Before the absorbance was measured, the baseline flatness and wavelength accuracy for the UV-spectrophotometer were carried out daily. The absorbance was measured using Milli-Q water as background and the concentration of dye was computed from calibration curves preliminary determined at different pHs. If the reading of absorbance was greater than 3.0, then the necessary dilution was made. After every experiment, the precision cell (10.00 mm, quartz SUPRASIL® (Hellma GmbH & Co., Germany)) was cleaned by soaking with methanol (HPLC Grade, Fischer Scientific UK Ltd., United Kingdom) overnight. The values of the initial and final concentrations of the dye measured as outlined above were used to calculate the removal percentage of the dye using Eq. (4).

$$\text{Dye removal}(\%) = 100 \times \frac{C_0 - C_f}{C_0} \tag{4}$$

where: C_0 is the initial dye concentration and C_f is the permeate dye concentration.

Total organic carbon (TOC) content was analysed by TOC analyser with autosampler (ASI-V) (Model TOC-VCPH, Shimadzu). For estimation of dye's isoelectric point (IEP), the pH metre was placed in the dye solution (100 mg/l) while stirring [51]. Then the 0.001 M HCl was added, the volume of HCl and the solution pH was recorded. The isoelectric point (IEP) observed was around 7.0 [52].

3. Results and discussion

3.1. Coagulation/flocculation–sand filtration (CF–SF) and nanofiltration (NF) performance

The molecule structure for C.I. Acid Black 210 dye is shown in Fig. 2. It contains three azo bonds (–N═N–) and other functional groups: amino (–NH_2), hydroxyl (–OH), nitro (–NO_2) and sodium/potassium salt of sulphonic acid (–SO_3Na).

The full UV spectrum for untreated and treated dye is given in Fig. 3. It can be seen from this figure that there are three distinctive peaks (λ_{max}) i.e. 315, 460 and 610 nm. Similar full UV spectrum for non-purified C.I. Acid Black 210 dye also have been observed by other works [28,18].

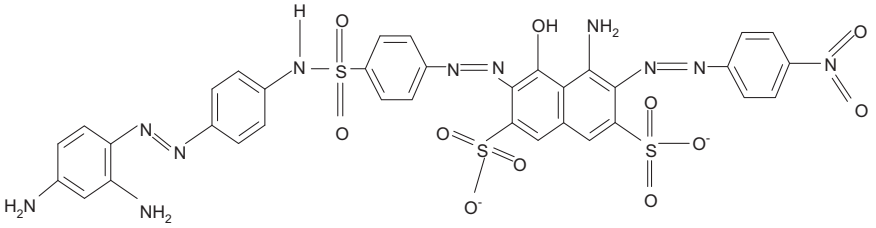

Fig. 2. Chemical formula for C.I. Acid Black 210 dye. (Reference: http://www.chemblink.com/products/99576-15-5.htm.)

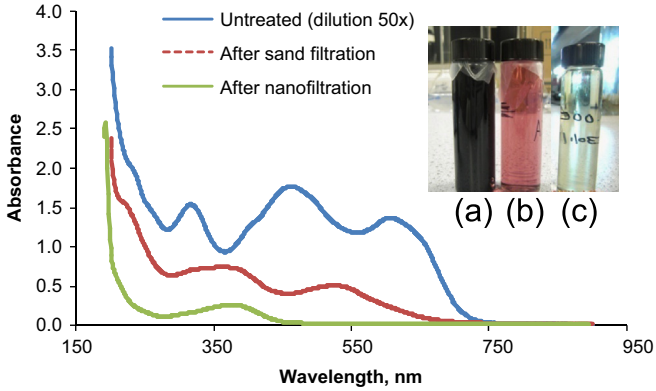

Fig. 3. UV–vis spectrum image of raw dye solution, permeate after CF–NF and NF. Picture attached shows (a) raw dye solution (b) CF–SF permeate (c) NF permeate.

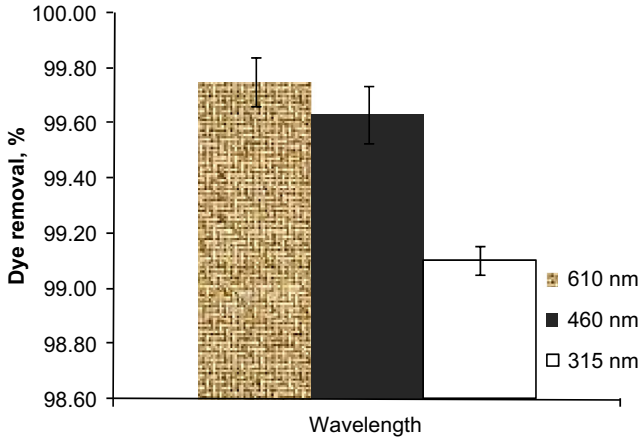

Fig. 4. Dye removal based on 315, 460, and 610 nm after coagulation/flocculation–sand filtration (Aluminium sulphate: 2 g/l, polymer: 7 mg/l, loading rate: 0.6 m^3/m^2 h, height of media: 325–375 mm, sand size: 0.3–0.6 mm)—error bar refer to standard deviation for triplicate measurements.

Generally, the peak of around 315 nm might be indicates the presence of small unsaturated compounds e.g. naphthalene [18,31] while the peaks of 460 and 610 nm might be due to the medium and large size unsaturated compounds, respectively [14]. From Fig. 3, the displacement of peaks 315 and 460 nm to high wavelengths for CF–SF and NF probably due to aggregation effect as been reported by Dragan and Dinu [20].

Complete disappearance of peak 610 nm for CF–SF and NF might be due to higher interaction between coagulant and/or sand surface and nanofiltration surface towards larger dye molecules [9]. However, incomplete disappearance of peak 315 and 460 nm might be due to the presence of low molecular mass impurities.

In order to choose suitable peak for estimating dye removal, the CF–SF permeate was investigated. It is found that the dye removal based on 315, 460 and 610 nm is 99.1%, 99.6% and 99.7% respectively (Fig. 4).This result suggests that absorbance at 315 nm can be a good estimator for the residual as it estimates the lowest removal of dye, which is in accordance with findings by Costa et al. [18].

From Table 1, the pH for CF–SF and NF permeate were around 4 and 8, respectively. The acidic SF permeate is due to the presence of aluminium ions. In aqueous solution, Al^{3+} is strongly hydrated and found surrounded by six co-ordinated water molecules in an octahedral configuration. The high

Table 1
Raw dye solution (4 g/l) and permeate characteristics after coagulation/flocculation–sand filtration (CF–SF) and nanofiltration (NF).

	Raw dye solution	CF–SF[a]	NF[b]
pH	9.2	4.0	8.3
Appearance	Black	Red	Slightly greenish
Dye, mg/l	4000	36	12
TOC, mg/l	1120	21	3
Conductivity, m s/cm	4.9	8.1	1.1

[a] CF–SF conditions: aluminium sulphate: 2 g/l, polymer: 7 mg/l, loading rate: 0.6 m^3/m^2 h, height of media: 325–375 mm, sand size: 0.3–0.6 mm, solution pH = 5.7.
[b] NF conditions: inlet pressure = 4.7 bar, solution pH = 10.0.

positive charge on the central metal ion causes some polarisation of the O–H bonds and there is a tendency for protons to dissociate giving one or more hydroxylated species. Therefore the complexes of Al ions in water act as weak acids [13].

Contrarily, the NF permeate pH is around 8.3 which is acceptable for water reuse [55]. It should be stated that the pH feed (raw dye solution) is around 10. However, due to the highly concentrated of dye; the charge effect have been reduced and hence the hydroxide ion (OH^-) repulsion is low. In this way, the OH^- could pass through the membrane.

Permeate colour is important for discharging effluent as well as for water reuse. From this study, it appears that the permeate colour depends on each treatment. It can be observed that the SF and NF permeate is dark red and slightly greenish, respectively (Table 1). The red colour might be due to the formation of stable aluminium–sulphonic acid complexes [36] during chelation/complexation reaction [33]. In another study, Costa et al. [18] found that pale yellow colour observed after C.I. Acid Black 210 dye was oxidised using electrochemical oxidation. Earlier, Zahrim et al. [54] has proposed the physicochemical reactions that occur during dye coagulation in an acidic pH as:

- Charge neutralisation due to aluminium hydrolysis product binding to the anionic sites such as sulpho, amino and hydroxy groups in the dye molecule.
- Adsorption of the dye molecule on the amorphous metal hydroxide precipitates via van der Waals interactions, hydrogen bonding etc.
- Complexation between the aluminium (III) and the dye molecules.

It can be observed that the residual dye at CF–SF permeate is higher than at NF permeate as shown in Table 1. Although, the flocculated dye could attach to the grain surface and the existing deposits [43], not all dye molecules tend to precipitate and become flocs. The soluble complexes could pass through the sand filter and consequently appear in the SF permeate. Apart from that, the attached flocs could be broken when the stress upon them is greater than their inter-flocs bond [24]. A study reported that the inter-flocs bond can be improved using high charge density and high molecular mass polymer [8]. The main mechanism for NF is sieving and surface charge effect, but at higher dye concentration (which also contains a higher salt concentration), the surface charge effect is reduced causing some of dye molecules to penetrate through the membrane layer. Using lower concentration of dye as feed i.e. 100 mg/l, NF could reduce the dye to a final concentration of 1.2 mg/l (Zahrim et al., 2013).

The total organic carbon (TOC) at CF–SF and NF permeate were 21 mg/l and 3 mg/l, respectively (Table 1) [57]. 12 mg dye/l contributes to 3 mg TOC/l, then 36 mg dye/l supposed to be 9 mg TOC/l. However, the TOC for CF–SF permeate was much higher than the expected value (12 mg TOC/l more). Therefore, the high TOC for CF–SF permeate is most probably due to the accumulation of unreacted polymer in the permeate [16,40] as well as non-coagulated dye molecules. In another study, Polasek and Mutl, [40] reported that the content of organohalogen increased by 40% when polyDADMAC was

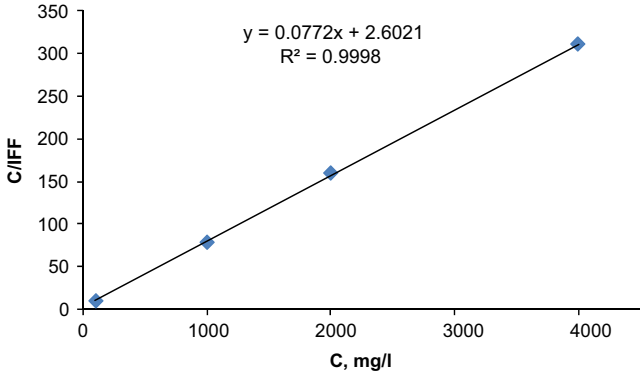

Fig. 5. Plotting of *C*/IFF vs. *C*.

added as flocculant for water treatment. A report during sludge dewatering stated that the application of high dosage of polymer would contribute to high residual polymer [34].

There is an increase in conductivity for CF–SF from 7.39 to 8.10 mS/cm (Table 1) which is due to presence of unreacted aluminium sulphate [30]. On the other hand, the NF permeate conductivity is 1.1 mS/cm. This result agrees with the finding of Petrinic et al., [39] who studied nanofiltration of printing dye wastewater. They reported that the conductivity removal was greater than $>80\%$ with initial conductivity of 2.74–3.77 mS/cm. For an ideal process, the water conductivity should be less than 1 mS/cm to avoid low quality dyed fabric [3].

Relationship between fouling factor (IFF) and initial concentration of dye (C) can be written as follows [57]:

$$\frac{C}{IFF} = \frac{1}{IFF_{\max}} C + \frac{1}{IFF_{\max} b} \tag{5}$$

By plotting (C/IFF) *vs. C* as shown in Fig. 5, the FF_{max} and b were found to be 12.95% and 0.0297 l/mg [57]. Gomes et al., [21] found that the affinity for C.I Acid Orange 7 towards polyamide membranes is 0.025 l/mg which is similar to values reported here.

Separation factor, R_L can also indicate the level of adsorption [42]. R_L is defined as:

$$R_L = \frac{1}{1 + bC_0} \tag{6}$$

where b is the Langmuir constant, C_0 the initial concentration of dye.
Value of R_L indicates several level of adsorption:
If $0 < R_L < 1$ indicates favourable adsorption.
If $R_L > 1$ indicates unfavourable adsorption.
If $R_L = 0$ indicates irreversible adsorption.
If $R = 1$ indicates linear adsorption.

In this study, the R_L for initial concentrations of 100 mg/l, 1000 mg/l, 2000 mg/l and 4000 mg/l were 0.252, 0.033, 0.017 and 0.008 respectively; which indicates favourable adsorption for initial concentration 100 mg/l while irreversible adsorption for initial concentration of 1000 mg/l, 2000 mg/l and 4000 mg/l. Adsorption of dye towards membrane surface could be due to van der Waals, hydrogen bond, dipole–dipole, hydrophobic interaction, ionic and covalent bond. However, chemical adsorption (ionic and covalent bond) is normally irreversible [4]. Van der bruggen et al. [44] reported that the irreversible fouling for strong acid dye bath is 34%–45% depending on pore size and at higher pore size i.e. 0.8 nm, no product flux was obseved. The variation in irreversible fouling might be due to the presence of auxiliary chemicals such as foam reducing agent, egaliser etc as well as the nanofiltration system used.

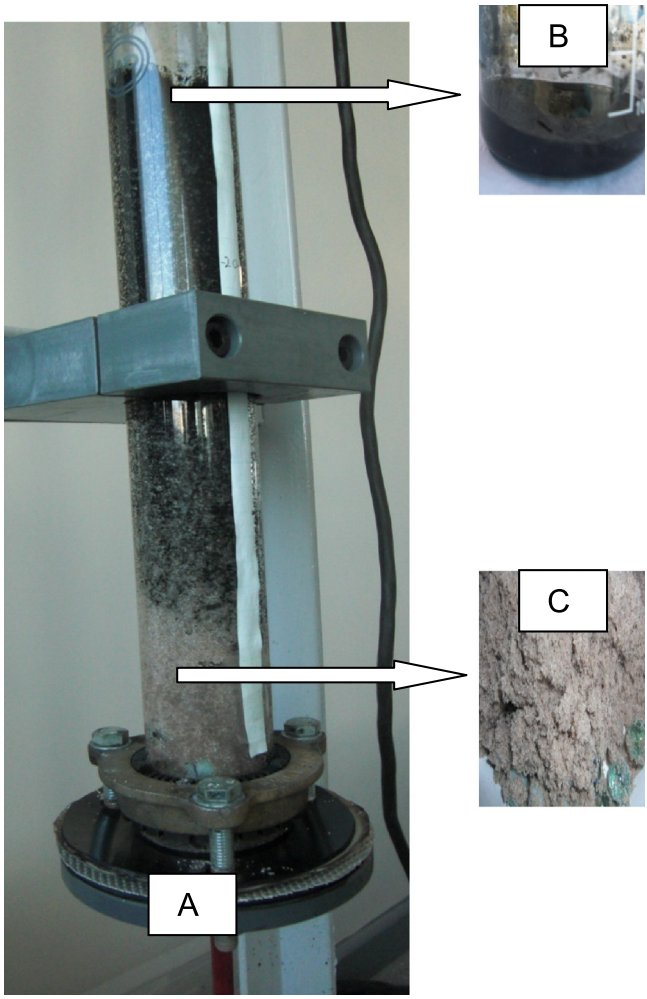

Fig. 6. Distribution of coagulated dye along the sand bed (A), the upper part (B) and the bottom part (C) (aluminium sulphate: 2 g/l, polymer: 7 mg/l, loading rate: 0.6 m^3/m^2 h, media height: 375 mm, sand size 0.3–0.6 mm).

It can be concluded from this work that both systems cannot be used alone to produce reusable water due to inability to produce colourless water. Based on several permeate parameters i.e. pH, residual dye, TOC and conductivity, it seems that NF is better than CF–SF for pre-treatment of highly concentrated dye. NF as a second stage might be used as a possible post treatment. Fouling is the major obstacle for implementation of NF. Therefore, a study of NF fouling during dye filtration is presented in this work. CF–SF may be employed as a pre-treatment for NF [56]. Breakthrough is an important parameter for sand filtration since it determines the operating time before the sand needs to be replaced. A breakthrough stage could be identified by the decline of the effluent quality or excessive head loss-blockage which reduces the filtration rate [13].

3.2. Sand filtration breakthrough

The loading rate for the sand filter was designed in this work to be 0.6 m^3/m^2 h was similar to the work of Visscher, [47]. From an engineering perspective, a higher loading rate is desirable for treating larger amount of wastewater due to a smaller footprint.

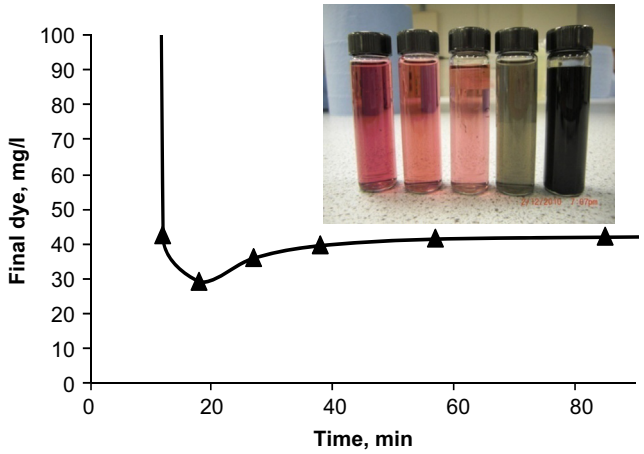

Fig. 7. Dye residual (based on 315 nm) for sand filtration treatment of coagulated dye small picture: from left to right—dye residual at filtration time of 38 min, 27 min, 18 min, 12 min and initial dye solution.

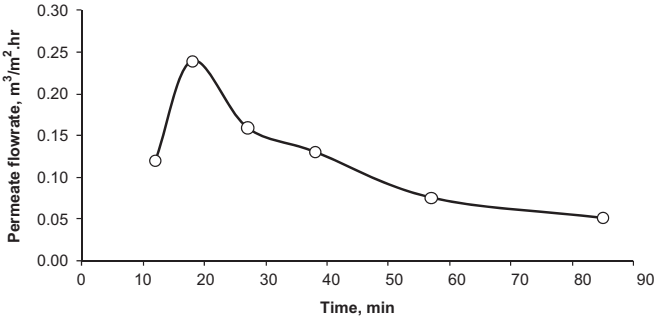

Fig. 8. Breakthrough for coagulated dye solution during sand filtration treatment (aluminium sulphate: 2 g/l, polymer: 7 mg/l, loading rate: 0.6 m^3/m^2 h, media height: 375 mm, sand size 0.3–0.6 mm).

It can be seen from Fig. 6 that most of the dye retained at the upper part of the sand filtration unit and the concentration is reduced along the column. This distribution is similar for the carbon distribution for slow sand filter that has been reported by Wotton [50]. Fig. 7 shows the evolution for the permeate dye concentration and the colour appearance during acid dye filtration (inset). From Fig. 7 (inset), it can be observed that at 12 min the colour is slightly black. After that the colour turned light red followed by a darker red appearance at the end of the experiment, which might be due to the breakage of retained flocs at the sand grain surface. By applying the optimum conditions for coagulation/flocculation–sand filtration, the recorded filtration rate was ~0.1–0.24 m^3/m^2.hr (Fig. 8) which can be classified as slow sand filtration [46].

Typically, the removal processes within sand filters comprise three stages: a working-in stage (characterised by a rapid decrease in effluent colour with time, reaching a low, stable value), a working stage (the effective (main) stage of filtration giving satisfactory effluent quality) and a breakthrough stage [13]. Fig. 8 shows that the working-in stage for the sand filtration was about 20 min. Initially, the rapid dye removal might be due to sand grain surface attachment. As the deposit builds up, the pore between sand grains become narrower, therefore, further drop in final dye concentration in the filtrate at 20 min of filtration time was observed. This process is called “ripening” process and the dye removal might be due to attachment to the deposit as well as sieving. After ripening, the final dye concentration in the filtrate increases slowly and then, the final dye concentration reached steady concentration at ~40 mg/l. This might be due to the

attachment–detachment mechanism in which the increase in hydraulic shear resulting from attachment of particles in a given layer of the bed leads to detachment and deposition in a subsequent layer until effluent quality decline occurs [23]. In this study, the decline of quality i.e. final dye concentration in the filtrate > 40 mg/l is not observed but the filtration rate showed a decline.

During 12 min of filtration, it was determined that the flow rate was ~0.13 m^3/m^2 h and then it was increased to 0.24 m^3/m^2 h. This occurred due to blockage causing an increase in the local velocity due to narrower pore space. Then, the filtration rate gradually declined until it reached 0.1 m^3/m^2 h at ~45 min filtration (Fig. 8). Therefore the breakthrough can be estimated at around 45 min.

4. Conclusions

Treatment of highly concentrated dye solution using CF–SF and NF has been studied. It can be concluded that hybrid treatment system is vital since none of the treatment able to fully decolourise the dye solution. For NF, pore blocking and concentration polarisation are major contributors for flux decline at higher dye concentration. Finally, the sand filtration breakthrough after coagulation/flocculation is estimated at around 45 min. Future works on alum and polymer dosage concentration optimisation to reduce conductivity and TOC are necessary.

Acknowledgements

Authors would like to thank the Universiti Malaysia Sabah and the Ministry of Higher Education, Malaysia for funding this work.

References

[1] A. Akbari, J.C. Remigy, P. Aptel, Treatment of textile dye effluent using a polyamide-based nanofiltration membrane, Chemical Engineering and Processing 41 (2002) 601–609.
[2] M.H. Al-Malack, Technical and economic aspects of crossflow microfiltration, Desalination 155 (2003) 89–94.
[3] M.I. Alcaina-Miranda, S. Barredo-Damas, A. Bes-Pia, M.I. Iborra-Clar, A. Iborra-Clar, J.A. Mendoza-Roca, Nanofiltration as a final step towards textile wastewater reclamation, Desalination 240 (2009) 290–297.
[4] S.J. Allen, B. Koumanova, Decolourisation of water/wastewater using adsorption (review), Journal of the University of Chemical Technology and Metallurgy 40 (2005) 175–192.
[5] Y. Anjaneyulu, N.S. Chary, D.S.S. Raj, Decolourization of industrial effluents—available methods and emerging technologies—a review, Reviews in Environmental Science and Bio/Technology 4 (2005) 245–273.
[6] J. Balasubramanian, P.C. Sabumon, J.U. Lazar, R. Ilangovan, Reuse of textile effluent treatment plant sludge in building materials, Waste Management 26 (2006) 22–28.
[7] P. Banerjee, S. Dasgupta, S. De, Removal of dye from aqueous solution using a combination of advanced oxidation process and nanofiltration, Journal of Hazardous Materials 140 (2007) 95–103.
[8] E. Barbot, S. Moustier, J.Y. Bottero, P. Moulin, Coagulation and ultrafiltration: understanding of the key parameters of the hybrid process, Journal of Membrane Science 325 (2008) 520–527.
[9] J. Beltran-Heredia, J.S. Martin, Azo dye removal by Moringa oleifera seed extract coagulation, Coloration Technology 124 (2008) 310–317.
[10] J. Beltran-Heredia, J. Sanchez-Martin, A. Delgado-Regalado, Removal of carmine indigo dye with moringa oleifera seed extract, Industrial and Engineering Chemistry Research 48 (2009) 6512–6520.
[11] A. Bes-Pia, M.I. Iborra-Clar, A. Iborra-Clar, J.A. Mendoza-Roca, B. Cuartas-Uribe, M.I. Alcaina-Miranda, Nanofiltration of textile industry wastewater using a physicochemical process as a pre-treatment, Desalination 178 (2005) 343–349.
[12] W.R. Bowen, T.A. Doneva, Atomic force microscopy studies of nanofiltration membranes: surface morphology, pore size distribution and adhesion, Desalination 129 (2000) 163–172.
[13] J. Bratby, Coagulation and Flocculation in Water and Wastewater Treatment, IWA Publishing, London, 2006.
[14] P.Y. Bruice, Organic Chemistry, Pearson International Edition, London, 2007.
[15] C.A. Buckley, A.E. Simpson, Effluent Treatment (1988). United States Patent. Patent No. 4752363.
[16] E.E. Chang, P.C. Chiang, W.Y. Tang, S.H. Chao, H.J. Hsing, Effects of polyelectrolytes on reduction of model compounds via coagulation, Chemosphere 58 (2005) 1141–1150.
[17] C.J. Chuang, K.Y. Li, Effect of coagulant dosage and grain size on the performance of direct filtration, Separation and Purification Technology 12 (1997) 229–241.
[18] C.R. Costa, F. Montilla, E. Morallón, P. Olivia, Electrochemical oxidation of Acid Black 210 dye on the boron-doped diamond electrode in the presence of phosphate ions: effect of current density, pH, and chloride ions, Electrochimica Acta 54 (2009) 7048–7055.
[19] E. Diamadopoulos, C. Vlachos, Coagulation-filtration of a secondary effluent by means of pre-hydrolyzed coagulants, Water Science and Technology 33 (1996) 193–201.

[20] E.S. Dragan, I.A. Dinu, Removal of azo dyes from aqueous solution by coagulation/flocculation with strong polycations, Research Journal of Chemistry and Environment 12 (2008) 5–11.
[21] A.C. Gomes, I.C. Goncalves, M.N. De pinho, The role of adsorption on nanofiltration of azo dyes, Journal of Membrane Science 255 (2005) 157–165.
[22] N. Hilal, G. Busca, N. Hankins, A.W. Mohammad, The use of ultrafiltration and nanofiltration membranes in the treatment of metal-working fluids, Desalination 167 (2004) 227–238.
[23] G.E. Jackson, Granular Media Filtration In Water And Wastewater-Treatment Part 2, CRC Critical Reviews in Environmental Control 11 (1980) 1–36.
[24] P. Jarvis, B. Jefferson, J. Gregory, S.A. Parsons, A review of floc strength and breakage, Water Research 39 (2005) 3121–3137.
[25] M. Khayet, A.Y. Zahrim, N. Hilal, Modelling and optimization of coagulation of highly concentrated industrial grade leather dye by response surface methodology, Chemical Engineering Journal 167 (2011) 77–83.
[26] I. Koyuncu, D. Topacik, E. Yuksel, Reuse of reactive dyehouse wastewater by nanofiltration: process water quality and economical implications, Separation and Purification Technology 36 (2004) 77–85.
[28] M. Li, J.T. Li, H.W Sun, Sonochemical decolorization of Acid Black 210 in the presence of exfoliated graphite, Ultrasonics Sonochemistry 15 (2008) 37–42.
[29] O. Marmagne, C. Coste, Color removal from textile plant effluents, American Dyestuff Reporter (April) (1996) 15–21.
[30] J.H. Mo, Y.H. Lee, J. Kim, J.Y. Jeong, J. Jegal, Treatment of dye aqueous solutions using nanofiltration polyamide composite membranes for the dye wastewater reuse, Dyes and Pigments 76 (2008) 429–434.
[31] M.Y.A. Mollah, J.A.G. Gomes, K.K. Das, D.L. Cocke, Electrochemical treatment of Orange II dye solution-Use of aluminum sacrificial electrodes and floc characterization, Journal of Hazardous Materials 174 (2010) 851–858.
[32] S.V. Mohan, N.C. Rao, P.N. Sarma, Simulated acid azo dye (Acid black 210) wastewater treatment by periodic discontinuous batch mode operation under anoxic-aerobic-anoxic microenvironment conditions, Ecological Engineering 31 (2007) 242–250.
[33] S.V. Mohan, P. Sailaja, M. Srimurali, J. Karthikeyan, Color removal of monoazo acid dye from aqueous solution by adsorption and chemical coagulation, Environmental Engineering and Policy 1 (1999) 149–154.
[34] Nunn, M., The effect of polymer dose on residual and toxicity in dewatering effluent. In*:* TAPPI Environmental Conference, 2000, Denver.
[36] E.G. Owens II, J.H. Yoe, Spectrophotometric determination of aluminum with 2-quinizarinsulfonic acid (sodium salt), Analytical Chemistry 31 (1959) 384–387.
[37] G. Ozdemir, B. Pazarbasi, A. Kocyigit, E.E. Omeroglu, I. Yasa, I. Karaboz, Decolorization of Acid Black 210 by *Vibrio harveyi* TEMS1, a newly isolated bioluminescent bacterium from Izmir Bay, Turkey, World Journal of Microbiology and Biotechnology 24 (2008) 1375–1381.
[38] J. Pearson, F. Lu, K. Gandhi, Disposal of woul scouring sludge by composting, Autex Reseach Journal 4 (2004) 147–156.
[39] I. Petrinic, N.P.R. Andersen, S. Sostar-Turk, A.M. Le marechal, The removal of reactive dye printing compounds using nanofiltration, Dyes and Pigments 74 (2007) 512–518.
[40] P. Polasek, S. Mutl, Cationic polymers in water treatment Part 1: treatability of water with cationic polymers, Water SA 28 (2002) 69–82.
[41] K. Ranganathan, K. Karunagaran, D.C. Sharma, Recycling of wastewaters of textile dyeing industries using advanced treatment technology and cost analysis—case studies, Resources Conservation and Recycling 50 (2007) 306–318.
[42] M.M. Rao, D.K. Ramana, K. Seshaiah, M.C. Wang, S.W.C. Chien, Removal of some metal ions by activated carbon prepared from phaseolus aureus hulls, Journal of Hazardous Materials 166 (2009) 1006–1013.
[43] W.W. Shuster, L.K. Wang, Role of polyelectrolytes in filtration of colloidal particles from water and wastewater, Separation and Purification Methods 6 (1977) 153–187.
[44] B. Van der bruggen, G. Cornelis, C. Vandecasteele, I. Devreese, Fouling of nanofiltration and ultrafiltration membranes applied for wastewater regeneration in the textile industry, Desalination 175 (2005) 111–119.
[45] B. Van der bruggen, J. Schaep, D. Wilms, C. Vandecasteele, M. Van den bosch, Nanofiltration for removal of organic substances from waste water—application in the textile industry, Chemistry for the Protection of the Environment *3* (55) (1998) 127–133.
[46] S. Vigneswaran, C. Visvanathan, Water treatment processes: simple options, CRC Press, Inc., Boca Raton, florida, 1995.
[47] J.T. Visscher, Slow sand filtration—design, operation, and maintenance, Journal American Water Works Association 82 (1990) 67–71.
[48] J. Warczok, M. Ferrando, F. Lopez, C. Guell, Concentration of apple and pear juices by nanofiltration at low pressures, Journal of Food Engineering 63 (2004) 63–70.
[50] R.S. Wotton, Water purification using sand, Hydrobiologia 469 (2002) 193–201.
[51] X.U.O.L. Xula 2011, Titration curve of an Amino Acid [Online], (Accessed 26.01.2011).
[52] A.Z. Yaser 2011. Development of Integrated Nanofiltration System for Highly Concentrated Dye Removal, Ph.D., Swansea University.
[54] A.Y. Zahrim, N. Hilal, C. Tizaoui, Evaluation of several commercial synthetic polymers as flocculant aids for removal of highly concentrated C.I. Acid Black 210 dye, Journal of Hazardous Materials 182 (2010) 624–630.
[55] A.Y. Zahrim, C. Tizaoui, N. Hilal, Coagulation with polymers for nanofiltration pre-treatment of highly concentrated dyes: a review, Desalination 266 (2011) 1–16.
[56] A.Y. Zahrim, C. Tizaoui, N. Hilal, Removal of highly concentrated industrial grade leather dye: Study on several flocculation and sand filtration parameters, Separation Science and Technology 46 (2011) 883–892.
[57] A.Y. Zahrim, N. Hilal, C. Tizaoui, Tubular nanofiltration of highly concentrated C.I. Acid Black 210 dye, Water Science and Technology 67 (2013) 901–906.